

1 Edge Removal in Random Contact Networks
2 and the Basic Reproduction Number

3 Dean Koch¹ Reinhard Illner²
4 and Junling Ma³

Department of Mathematics and Statistics, University of Victoria,
Victoria BC V8W 3R4, Canada

1 dk@uvic.ca

2 rillner@uvic.ca

3 corresponding to: junlingm@uvic.ca

5 May 8, 2012

6 **Abstract**

7 Understanding the effect of edge removal on the basic reproduction
8 number \mathcal{R}_0 for disease spread on contact networks is important for dis-
9 ease management. The formula for the basic reproduction number \mathcal{R}_0
10 in random network SIR models of configuration type suggests that for
11 degree distributions with large variance, a reduction of the average de-
12 gree may actually increase \mathcal{R}_0 . To understand this phenomenon, we
13 develop a dynamical model for the evolution of the degree distribu-
14 tion under random edge removal, and show that truly random removal
15 always reduces \mathcal{R}_0 . The discrepancy implies that any increase in \mathcal{R}_0
16 must result from edge removal changing the network type, invalidating
17 the use of the basic reproduction number formula for a random con-
18 tact network. We further develop an epidemic model incorporating a
19 contact network consisting of two groups of nodes with random intra-
20 and inter-group connections, and derive its basic reproduction num-
21 ber. We then prove that random edge removal within either group,
22 and between groups, always decreases the appropriately defined \mathcal{R}_0 .
23 Our models also allow an estimation of the number of edges that need
24 to be removed in order to curtail an epidemic.

25 **Keywords** network, SIR model, basic reproduction number, dis-
26 ease dynamics, edge removal, multi-group, network evolution

27 **Mathematics Subject Classification (2000)** 92D30

28 1 Introduction

29 The problem of mathematically describing the progression of an SIR disease
30 is usually simplified by assuming that individuals in the population are well
31 mixed [4]. Transmission events are then governed by a mass-action law, with
32 the underlying assumption that encounters between any two individuals in
33 the population occur with equal probability. Individuals belong to one of
34 three states: susceptible, infective, and removed/recovered with immunity;
35 the fraction of the population contained in each state is denoted by S , I , and
36 R , respectively. A pairing of (or contact between) individuals is sufficient for
37 the disease to jump from an infective to a susceptible, and all such pairings
38 are assumed to happen with equal likelihood. If β is the rate in time at which
39 pairings leading to infection occur, and γ is the rate of recovery, then the
40 familiar Kermack-McKendrick SIR model, which is a special case of a much
41 more general model presented in [7], is

$$42 \quad S' = -\beta SI, \quad I' = \beta SI - \gamma I, \quad R' = \gamma I. \quad (1)$$

43 However, in a real world population certain pairings almost never happen,
44 while other pairings are exceedingly common. Encounters between family
45 members, spouses, and friends, for example, are far more probable than the
46 average random pairing. By accounting for these close-knit connections in
47 the population structure, one can expect to model disease spread more re-
48 alistically. There are other pairings which occur less frequently but reliably,
49 for example encounters with doctors or nurses in a clinic or hospital. These
50 latter pairings become particularly important during an epidemic, and while
51 the rate of transmission for such pairings may be different from the rate
52 for more casual encounters, pairings with hospital employees cannot be pre-
53 vented during time of disease.

54 A contact network is a network representation of the contact structures
55 in a population, where individuals are represented by nodes, and if there
56 are contacts between two individuals, there is an edge connecting the two
57 corresponding nodes; see, for example, [13]. Following [13], we will call such

58 a random network a network of configuration type if there is a degree dis-
59 tribution P_k , $k = 0, 1, 2, \dots$ such that a randomly chosen network node (a
60 vertex) has, with probability P_k , k connections to other nodes. To construct
61 a random graph with these properties, first chose the desired number of ver-
62 tices N , then draw a degree sequence $\{k_i\}$ from the distribution and attach k_i
63 “stubs” to the i -th node. Finally, randomly choose pairs of these stubs from
64 two nodes that are not already neighbours, and connect them to form edges.
65 The process of stub connection is repeated until no edge can be formed. Any
66 remaining stubs are then discarded.

67 Disease threshold conditions, i.e., conditions that determine whether a
68 disease can invade a population, are of tremendous public health interest.
69 Traditionally, the basic reproduction number \mathcal{R}_0 , which is the average num-
70 ber of secondary infections caused by a typical infectious individual during
71 one’s course of infection in a completely susceptible population, is the most
72 commonly used one. Disease can invade if and only if $\mathcal{R}_0 > 1$. For network
73 models, another commonly used threshold is the critical transmissibility T_c .
74 Disease can invade if and only if the per edge transmission probability $T > T_c$.
75 Assuming exponentially distributed waiting times for transmission and re-
76 covery events, $T = \frac{\beta}{\beta + \gamma}$. For disease dynamics on configuration type contact
77 networks, the basic reproduction number \mathcal{R}_0 and the critical transmissibility
78 T_c are defined below.

79 Using bond percolation theory, Newman [13] studied the final state of an
80 epidemic on a random contact network of configuration type without degree
81 correlation or clustering. The critical transmissibility was shown to be

$$82 \quad T_c = \frac{\langle k \rangle}{\langle k^2 \rangle - \langle k \rangle}.$$

83 Newman further found that the disease may cause an epidemic if and only
84 if the transmissibility along an edge is large enough, which is equivalent to
85 $\mathcal{R}_0 > 1$, where

$$86 \quad \mathcal{R}_0 = T \left(\frac{\langle k^2 \rangle}{\langle k \rangle} - 1 \right) = T \left(\langle k \rangle - 1 + \frac{\text{Var}[k]}{\langle k \rangle} \right). \quad (2)$$

87 Here $\langle k \rangle$, $\langle k^2 \rangle$, and $\text{Var}[k] = \langle k^2 \rangle - \langle k \rangle^2$ are the average, the second moment,
88 and the variance of the degree distribution. Note that, at the beginning
89 of an epidemic on a random network, because the degree distribution of
90 a node found by following a random edge is $\{kP_k/\langle k \rangle\}$ where P_k is the

91 network degree distribution, the factor inside the parentheses is the average
 92 number of transmissible neighbors of the node after it is infected by one of its
 93 neighbors. Thus \mathcal{R}_0 is the basic reproduction number. Equation (2) shows
 94 that, in contact network models, \mathcal{R}_0 depends on both the transmissibility
 95 and the degree distribution. $\mathcal{R}_0 > 1$ is equivalent to the transmissibility
 96 threshold condition

$$97 \quad T > T_c = \frac{\langle k \rangle}{\langle k^2 \rangle - \langle k \rangle}.$$

98 The first model describing the disease dynamics on contact networks was
 99 developed by Pastor-Satarrass and Vespignani [15] and is related to work of
 100 Anderson and May [10]. The Pastor-Satarrass and Vespignani model divides
 101 the population into degree classes (the number of contacts that an individual
 102 has), and assumes random mixing among these classes. It yields a larger ba-
 103 sic reproduction number than (2), and thus predicts a faster growth of disease
 104 epidemic, because this model does not consider the fact that the disease can-
 105 not transmit along an edge more than once until one of its nodes recovers and
 106 becomes susceptible again. A few extensions of this model (see, for example,
 107 [1, 9], keep track of the number of “effective” (i.e., transmissible) neighbors,
 108 and yield basic reproduction numbers as in (2). These models employ a large
 109 number of equations and are therefore difficult to analyze. For SIR epidemics,
 110 Volz [17] developed a much simpler model tracking the number of edges that
 111 connect nodes of different infection status. This model was further simplified
 112 by Miller [12], who arrived at an effectively one-dimensional model. Both
 113 models yield basic reproduction numbers equivalent to (2). These papers
 114 thus confirm that, under the assumption of random contact networks with
 115 no degree correlation and clustering, the basic reproduction number of an
 116 SIR epidemic is given by (2). Lindquist et al. [9] showed that for diseases
 117 with no acquired immunity (SIS), the disease threshold is different from
 118 (2). However, for simplicity, in this present work we restrict ourselves to SIR
 119 epidemics.

120 It is a question of some significant practical relevance how the basic re-
 121 production number will behave if the network is altered. These alteration
 122 may be caused by finding or losing friends, a change of jobs, or more in-
 123 terestingly, interventions such as vaccination, isolation and quarantine, and
 124 social distancing. It is a challenge to study the disease spread on an evolving
 125 network, because of the coupling of the disease dynamics and the network
 126 evolution dynamics. In this paper, we study the effect of dropping contacts
 127 (edges) before an epidemic. Doing so effectively decouples the two dynamics.

128 Because the transmission probability T is independent of the network struc-
 129 ture, Equation (2) shows that the change of \mathcal{R}_0 is determined by the change
 130 of $\langle k \rangle$ and $\text{Var}[k]$.

131 **1.1 Counterintuitive results from a simple analysis of** 132 **bi-modal networks: a paradox?**

133 Common sense states that R_0 should decrease as edges are severed (this
 134 is the basic tenet of quarantine and isolation). In other words, one would
 135 expect \mathcal{R}_0 to be an increasing function of the average degree $\langle k \rangle$, and this
 136 is indeed true if the degree distribution of the random contact network is
 137 Poisson. In that case, $\langle k^2 \rangle = \langle k \rangle^2 + \langle k \rangle$, and $\mathcal{R}_0 = \frac{\beta}{\beta + \gamma} \langle k \rangle$. However, for
 138 other distributions this calculation does not apply. As x edges are randomly
 139 removed, $\langle k \rangle$ decreases with x . $\text{Var}[k]$ is also a function of x , and therefore

$$140 \quad \frac{d}{dx} \mathcal{R}_0 = T \left[\left(1 - \frac{\text{Var}[k]}{\langle k \rangle^2} \right) \frac{d}{dx} \langle k \rangle + \frac{1}{\langle k \rangle} \frac{d}{dx} \text{Var}[k] \right]. \quad (3)$$

141 This suggests that, if the variance of the degree distribution is kept constant,
 142 then \mathcal{R}_0 could increase when $\langle k \rangle^2 < \text{Var}[k]$, i.e., when the variance is large,
 143 dropping edges may accelerate the epidemic. In fact, this effect becomes
 144 exaggerated if $\text{Var}[k]$ increases with edge removal.

145 To illustrate this possibility we present a simple example of a network
 146 with bimodal degree distribution, i.e., a fraction p of the nodes with degree
 147 k_1 , the other $(1 - p)$ with degree $k_2 > k_1$. Assuming that T and p remain
 148 constant, we ask how \mathcal{R}_0 responds to changes in k_1 and k_2 in the following
 149 two scenarios.

150 **1.1.1 Constant variance**

151 Let k_1 and k_2 both increase by the same amount, keeping $d = k_2 - k_1$ constant.
 152 Consequently, the variance, $\text{Var}[k] = d^2 p(1 - p)$ stays constant while the
 153 average degree increases.

154 Using $k_2 = k_1 + d$, we can write Equation (2) as

$$155 \quad \mathcal{R}_0 = T \left(\frac{k_1^2 p + (k_1 + d)^2 (1 - p)}{k_1 p + (k_1 + d)(1 - p)} - 1 \right)$$

156 As we are interested only in the sign of $\frac{\partial \mathcal{R}_0}{\partial k_1}$, we discard the positive-valued
 157 factors T and the denominator of the derivative after differentiation. This

158 yields

$$\begin{aligned}
 159 \quad \frac{\partial}{\partial k_1} \mathcal{R}_0 &\propto 2[k_1 + d(1-p)]^2 - [k_1^2 p + (k_1 + d)^2(1-p)] \\
 160 \quad &\propto k_1^2 + 2k_1 d(1-p) + d^2(1-p)(1-2p). \\
 161
 \end{aligned}$$

162 We can read off this formula that \mathcal{R}_0 decreases with $k_1 > 0$ if $p > 1/2$ and

$$163 \quad 0 < k_1 < d \left[(p-1) + \sqrt{p(1-p)} \right].$$

164 Note that the right hand side is positive if $p > 1/2$. Conversely, \mathcal{R}_0 will
 165 increase as k_1 decreases inside the computed range.

166 1.1.2 Constant high degree

167 Here we let k_1 change, while k_2 is held constant. Thus, the standard deviation
 168 increases linearly with k_1 , while the variance $(k_2 - k_1)^2 p(1-p)$ increases.
 169 Again, we have

$$170 \quad \mathcal{R}_0 = T \left(\frac{k_1^2 p + k_2^2(1-p)}{k_1 p + k_2(1-p)} - 1 \right)$$

171 and as we increase k_1 ,

$$172 \quad \frac{\partial}{\partial k_1} \mathcal{R}_0 \propto k_1^2 p^2 + 2k_1 k_2 p(1-p) - k_2^2 p(1-p)$$

173 a quadratic in k_1 . Thus, \mathcal{R}_0 decreases with increasing $k_1 > 0$ if

$$174 \quad k_1 < k_2 \frac{\sqrt{1-p} - (1-p)}{p}.$$

175 We found that by manipulating the edge distribution in certain ways,
 176 \mathcal{R}_0 as defined above can increase in value despite a decreasing $\langle k \rangle$. This
 177 contradicts the basic tenet of quarantine — or does it? By decreasing the
 178 total number of edges in the network we are, in a sense, limiting the number
 179 of paths available to the disease, so one would expect a reduced growth rate.
 180 We leave the resolution of this paradox to the end of the paper, but give
 181 a hint. The problem with the above reasoning is that the removal of edges
 182 subject to the rules given above leaves us with networks which are no longer
 183 configuration type (see the discussion at the end), and in a network which

184 is not of this class, R_0 as defined above is no longer the basic reproduction
185 number — one has to use a different definition.

186 In Section 2 we provide an argument which shows that R_0 will always
187 decrease if the edge removal is truly random. In fact, we can show that
188 Newman’s R_0 is a Lyapunov functional for the system relative to a variable
189 measuring random edge removal.

190 In Section 3 we extend the Miller network SIR model [11] to describe a
191 population split into two subnetworks in order to allow random edge removal
192 from just a subset of the entire population. We then derive the basic re-
193 productive number \mathcal{R}_0 for the model and prove that \mathcal{R}_0 will indeed always
194 decrease under random edge removal. The result from Section 2 is a critical
195 ingredient in this analysis.

196 In summary, the conclusion of our work is that the basic tenet of quaran-
197 tine holds rigorously for the models under consideration, and that conceivable
198 exceptions are based on logical errors as are common in probabilistic models.
199 We have chosen to include this “paradox” for motivational and pedagogical
200 reasons.

201 **2 Random edge removal in a random network**

202 In this section we discuss random edge removal and its effect on the disease
203 dynamics. Here we discuss two processes: one is to simply uniformly choose
204 an edge for removal, the other is to first uniformly choose a node (disregarding
205 its degree) and then uniformly choose one of its edges for removal. In the
206 latter approach the edges are not uniformly chosen for removal. In fact, edges
207 of low degree nodes will have a larger probability for removal than edges of
208 high degree nodes. However, the second scenario may be more relevant for
209 disease dynamics, as edge removal decisions are normally individual based
210 rather than edge based.

211 **2.1 Uniform edge removal**

212 Assume that a fraction p of the edges will be removed. Because we assume
213 that these edges are uniformly chosen for removal, each edge removal is thus a
214 Bernoulli trial with success probability p . Assuming that the contact network
215 has a degree distribution P_k (i.e., the probability that a node has degree k is

216 P_k), its probability generating function is

$$217 \quad G(x) = \sum_{k=0}^{\infty} x^k P_k,$$

218 After the removal, the probability generating function for the degree distri-
219 bution is then

$$220 \quad G_r(x) = G(p + x(1 - p))$$

221 Thus, after removal, the average degree is

$$222 \quad \langle k \rangle_r = \frac{d}{dx} G_r(1) = (1 - p) G'(1) = (1 - p) \langle k \rangle,$$

223 where $\langle k \rangle$ is the average degree before removal. In addition, the second
224 moment is

$$225 \quad \langle k(k - 1) \rangle_r = \frac{d^2}{dx^2} G_r(1) = (1 - p)^2 G''(1) = (1 - p)^2 \langle k(k - 1) \rangle.$$

226 Thus, the basic reproduction number \mathcal{R}_0 as a function of the removal prob-
227 ability p is

$$228 \quad \mathcal{R}_0(p) = \frac{\beta}{\beta + \gamma} \frac{\langle k(k - 1) \rangle_r}{\langle k \rangle_r} = (1 - p) \frac{\beta}{\beta + \gamma} \frac{\langle k(k - 1) \rangle}{\langle k \rangle}$$

229 which is a decreasing function of p . That is, truly random edge removal
230 reduces \mathcal{R}_0 .

231 **2.2 Edge removal of a random node**

232 When a random edge of a uniformly chosen node is removed, the above
233 moment generating function method cannot be easily applied. In this case,
234 we develop a model for the dynamics of degree distribution with edge removal.

235 Given the transmission probability T along an edge, the basic reproduc-
236 tion number (2) is only a function of the network degree distribution N_k (the
237 *number* of nodes of degree k). We thus need to model how degree distribution
238 evolves with edge removal. Let $N = \sum_{k=0}^{\infty} N_k$ be the total number of nodes,
239 and $L = \sum_{k=0}^{\infty} k N_k$ be the sum of degrees (twice the number of edges) in the
240 network. Here we use a simplified network evolution model [8] to describe

241 the evolution of the network degree distribution. For simplification, we pick
 242 the time scale such that the edge removal process occurs with rate one.

243 The probability that a random node of nonzero degree, selected for edge
 244 removal, has degree $k \geq 1$ is $N_k/(N - N_0)$. Having selected one of its edges,
 245 the probability that the neighbor has degree $k \geq 1$ is proportional to the
 246 sum of the degrees of all nodes in N_k , i.e., kN_k/L . Both nodes reduce their
 247 degree by one, thus entering N_{k-1} if they are in N_k . Hence, the dynamics of
 248 the degree distribution N_k can be modeled as

$$249 \quad \frac{d}{d\tau} N_k = \frac{1}{N - N_0} (N_{k+1} - N_k) + \frac{1}{L} [(k+1)N_{k+1} - kN_k], \quad k \geq 1, \quad (4)$$

$$250 \quad \frac{d}{d\tau} N_0 = \frac{N_1}{N - N_0} + \frac{N_1}{L}, \quad (5)$$

252 **2.3 The rate of change of the basic reproduction num-** 253 **ber**

254 From Equation (2),

$$255 \quad \mathcal{R}_0 = T \left(\frac{\langle k^2 \rangle}{\langle k \rangle} - 1 \right) = T \left(\frac{\sum_{k=0}^{\infty} k^2 N_k}{\sum_{k=0}^{\infty} k N_k} \right). \quad (6)$$

256 Using Equations (4) and (5), it can be derived that (see Appendix A),

$$257 \quad \frac{d}{d\tau} \mathcal{R}_0 = 2T \left(\frac{1}{L} - \frac{1}{N - N_0} \right) < 0. \quad (7)$$

258 In fact, because by definition τ is a measure of the number of edges
 259 removed, given that the initial total degree is $L(0)$, the total degree at time τ
 260 is $L(\tau) = L(0) - 2\tau$. During the initial phase of edge removal, the probability
 261 that a node loses all its edges is small, and thus N_0 can be treated as a
 262 constant. We can thus solve Equation (7) approximately for small τ ,

$$263 \quad \mathcal{R}_0(\tau) - \mathcal{R}_0(0) = -T \left[\log \left(1 - \frac{2\tau}{L(0)} \right) + \frac{2\tau}{N - N_0} \right]. \quad (8)$$

264 Note that this fails as a good approximation of \mathcal{R}_0 when N_0 becomes large.

265 Equation (7) shows that the basic reproduction number \mathcal{R}_0 will decrease
 266 under random edge removal. This holds for any random network without
 267 degree correlation and clustering, regardless of degree distribution. Thus

268 we find some disparity with the examples of bimodal degree distributions in
269 section 1.

270 Yet, for the first bimodal example, the number of edges removed from
271 the low and high degree nodes are proportional to $\Delta k_1 p$ and $\Delta k_1(1 - p)$,
272 respectively. Clearly, when $p > 0.5$, the number of edges removed from
273 the low degree nodes exceed those from high degree nodes. For the second
274 example where the high degree is fixed while the low degree is reduced, only
275 low-to-low edges can be removed. On the other hand, equations (4)–(5) are
276 only applicable for random edge removal from the whole network, i.e., every
277 node has the same probability to be selected for edge removal. We address
278 this problem in Section 3

279 **3 Edge removal from part of the network**

280 The apparent paradox presented at the end of Section 2 arises because the
281 unintuitive results presented in Section 1 are derived using the basic repro-
282 duction number formula suitable only for random contact networks generated
283 from configuration models, yet the edge removal scenarios presented in Sec-
284 tion 1 break the configuration model assumption. Thus, if we derive the
285 correct formula for \mathcal{R}_0 for contact networks that are not of configuration
286 model type, for example networks resulting from edge removal restricted to
287 a component of a network, we should still see \mathcal{R}_0 decrease with random edge
288 removal. In this section, we verify this conjecture.

289 We model edge removal from a network consisting of two groups of nodes,
290 A and B, with random intra- and inter-group edges. Let N_A and N_B be the
291 number of nodes in each group. For a node in group A, its edge is labeled
292 either AA or AB if it connects to a neighbor in group A or B, respectively.
293 The BB and BA edges are similarly labeled for target nodes in group B.
294 We assume that the intra- and inter-group connections are random with no
295 degree correlation. Further, for individual nodes, there must be no correlation
296 between the number of intra and inter-group edges. Since each connection
297 between group A and B is both of type AB and BA, the total number of AB
298 edges must equal the total number of BA edges.

299 We assume that edge removal in either group, and between groups, may
300 occur at different rates. In this section, we model the disease dynamics,
301 derive the basic reproduction number, and study the change of the basic
302 reproduction number with edge removal.

303 3.1 Disease dynamics

304 First we need to model the disease dynamics. We extend the Miller model
305 [11], which describes the SIR disease dynamics on a random network without
306 degree correlation and clustering, to two randomly connected subnetworks.

307 3.1.1 The Miller Model

308 Consider a susceptible node with degree k . This node remains susceptible
309 as long as none of its k edges has transmitted disease. Let $\theta(t)$ be the
310 probability that such an edge has not transmitted disease by time t , then
311 the probability that this node remains susceptible is θ^k . We are interested in
312 how fast this susceptible node becomes infected, which is solely determined
313 by the dynamics of θ . In addition, while this node remains susceptible,
314 the infection events along each edge are independent of each other. Thus, to
315 understand the dynamics of θ , we can restrict the analysis to one of its edges,
316 and assume that transmission can only be passed through this edge to the
317 susceptible node. That is, the edge can be considered as if it was connected
318 to a degree-1 susceptible node.

319 Let P_k be the degree distribution, which is generated by the probability
320 generating function

$$321 \Psi(x) = \sum_{n=0}^{\infty} x^n P_n. \quad (9)$$

322 Then the probability that a randomly selected node remains susceptible at
323 time t is $\Psi(\theta)$. Thus, the fraction of nodes that are susceptible at time t is

$$324 S = \Psi(\theta). \quad (10)$$

325 We now describe the dynamics of θ . Let $P_I(t)$ be the probability that the
326 neighbor connected by this edge is infectious at time t , and β be the trans-
327 mission rate along an random edge. Then βP_I is the attack rate on the edge,
328 and θ is the survival probability, thus,

$$329 \theta' = -\beta P_I \theta.$$

330 Let $\phi = P_I \theta$, which is the probability that a random edge connects a (degree-
331 1, see the paragraph above) susceptible node to an infectious node. Then,
332 the above equation becomes

$$333 \theta' = -\beta \phi. \quad (11)$$

334 We need to describe the dynamics of ϕ , i.e., the class of edges connecting
 335 a degree-1 susceptible node to a infectious node. An edge leaves class ϕ either
 336 because transmission occurred along it (with rate β), or the infectious node
 337 recovers (with rate γ). An edge of a susceptible node enters class ϕ because
 338 its other neighbor becomes infected, which happens at a rate $-h'(t)$, where
 339 $h(t)$ is the probability that we arrive at a susceptible node when following a
 340 random edge that has not transmitted disease. Thus,

$$341 \quad \phi' = -\beta\phi - \gamma\phi - h'(t).$$

342 We now model $h(t)$. Note that the probability that we arrive at a given
 343 node when following a random edge is proportional to its degree (because of
 344 the random network assumption). The probability that we arrive at a degree-
 345 k node is then $q_k = kP_k / \sum_{k=0}^{\infty} kP_k = kP_k / \Psi'(1)$. Thus, the probability that
 346 this node is susceptible is $\theta^{k-1}q_k$ and we arrive at

$$347 \quad h(t) = \sum_{k=0}^{\infty} \theta^{k-1} \frac{kP_k}{\Psi'(1)} = \frac{\Psi'(\theta)}{\Psi'(1)}. \quad (12)$$

348 The equation for ϕ' can now be rewritten as

$$349 \quad \phi' = -(\beta + \gamma)\phi - \frac{\Psi''(\theta)}{\Psi'(1)}\theta' = -(\beta + \gamma)\phi + \beta\phi \frac{\Psi''(\theta)}{\Psi'(1)}. \quad (13)$$

350 The dynamics of the disease are thus determined by (11) and (13). The
 351 fraction of nodes which are infectious at time t changes according to

$$352 \quad I'(t) = -S' - \gamma I = \beta\phi\Psi'(\theta) - \gamma I. \quad (14)$$

353 3.1.2 Our two-group model

354 We now extend the Miller model to describe the disease dynamics on our two-
 355 group network. Assume that, in this two-group network, the distribution P_{AA}
 356 of the number of AA edges attached to a node in group A is generated by
 357 the probability generating function $\Psi_{AA}(x)$, defined as

$$358 \quad \Psi_{AA}(x) = \sum_{i=0}^{\infty} P_{AA}(i)x^i,$$

359 The distributions P_{AB} , P_{BA} , and P_{BB} and their generating functions $\Psi_{AB}(x)$,
 360 $\Psi_{BA}(x)$ and $\Psi_{BB}(x)$ can be similarly defined. Thus, the balance condition
 361 equating the number of AB and BA edges can be written as

$$362 \quad N_A \Psi'_{AB}(1) = N_B \Psi'_{BA}(1), \quad (15)$$

363 where $\Psi'_{ij}(1)$, $i, j = A$ and B , are the average number of neighbors in each
 364 type.

365 Let α be the rate of transmission along edges between A and B ; β_A and β_B
 366 be the corresponding transmission rates within groups A and B , respectively.
 367 As before, we define γ to be the per-infective recovery rate.

368 For a susceptible node in group A , let $\theta_{AA}(t)$ be the probability that one
 369 of its edges has never transmitted disease by time t . The expression for θ_{AA}
 370 is similar to the Miller model. That is, if $\phi_{AA}(t)$ denotes the probability
 371 that an edge connected to a susceptible node in group A is connected to an
 372 infectious node and the edge has not transmitted disease, then

$$373 \quad \theta'_{AA} = -\beta_A \phi_{AA}, \quad (16)$$

374 and

$$375 \quad \phi'_{AA} = -(\beta + \gamma)\phi_{AA} - h'_{AA}(t),$$

376 where $h_{AA}(t)$ is the probability that we arrive at a susceptible node in group
 377 A when following a random AA edge.

378 However, the dynamics of h_{AA} must reflect the fact that a neighbor of
 379 a group A node can be in either group A or group B . By the independence
 380 assumption made on the intra- and inter-group connections, the generating
 381 function for the degree distribution of a given node in group A is the product
 382 of the generating functions for its AA and AB degree distributions. Thus,
 383 having followed a random AA edge to arrive at a different node in group A ,
 384 the probability that this node has i neighbors in A and j neighbors in B is

$$385 \quad \left[i P_{AA}(i) / \sum_{k=0}^{\infty} k P_{AA}(k) \right] P_{AB}(j),$$

386 and

$$387 \quad h_{AA}(t) = \left[\sum_{i=0}^{\infty} \theta_{AA}^{i-1} \frac{i P_{AA}(i)}{\sum_{k=0}^{\infty} k P_{AA}(k)} \right] \left[\sum_{j=0}^{\infty} \theta_{AB}^j P_{AB}(j) \right]$$

$$388 \quad = \frac{\Psi'_{AA}(\theta_{AA})}{\Psi'_{AA}(1)} \Psi_{AB}(\theta_{AB}).$$

389

390 Hence, the dynamics of ϕ_{AA} becomes

$$\begin{aligned}
391 \quad \phi'_{AA} &= -\gamma\phi_{AA} - \beta_A\phi_{AA} + [-h'_{AA}(t)] \\
392 \quad &= -\gamma\phi_{AA} - \beta_A\phi_{AA} + \beta_A\phi_{AA} \frac{\Psi''_{AA}(\theta_{AA})}{\Psi'_{AA}(1)} \Psi_{AB}(\theta_{AB}) + \\
393 \quad &\quad \alpha\phi_{AB} \frac{\Psi'_{AA}(\theta_{AA})}{\Psi'_{AA}(1)} \Psi'_{AB}(\theta_{AB}). \tag{17} \\
394
\end{aligned}$$

395 We can follow the same reasoning and derive the probability that an
396 edge of a group A susceptible node connected to a group B node has not
397 transmitted disease at time t , $\theta_{AB}(t)$, and the probability that an edge of a
398 susceptible group A node connected to an infectious node in group B yet has
399 not transmitted disease by time t , $\phi_{AB}(t)$. In like manner we define $\theta_{BA}(t)$,
400 $\phi_{BA}(t)$, $\theta_{BB}(t)$ and $\phi_{BB}(t)$.

$$401 \quad \theta'_{AB} = -\alpha\phi_{AB}, \tag{18}$$

$$402 \quad \theta'_{BA} = -\alpha\phi_{BA}, \tag{19}$$

$$403 \quad \theta'_{BB} = -\beta_B\phi_{BB}, \tag{20}$$

$$\begin{aligned}
404 \quad \phi'_{BB} &= -\gamma\phi_{BB} - \beta_B\phi_{BB} + \beta_B\phi_{BB} \frac{\Psi''_{BB}(\theta_{BB})}{\Psi'_{BB}(1)} \Psi_{BA}(\theta_{BA}) \\
405 \quad &\quad \alpha\phi_{BA} \frac{\Psi'_{BB}(\theta_{BB})}{\Psi'_{BB}(1)} \Psi'_{BA}(\theta_{BA}). \tag{21}
\end{aligned}$$

$$\begin{aligned}
406 \quad \phi'_{AB} &= -\gamma\phi_{AB} - \alpha\phi_{AB} + \alpha\phi_{BA} \frac{\Psi''_{BA}(\theta_{BA})}{\Psi'_{BA}(1)} \Psi_{BB}(\theta_{BB}) + \\
407 \quad &\quad \beta_B\phi_{BB} \frac{\Psi'_{BA}(\theta_{BA})}{\Psi'_{BA}(1)} \Psi'_{BB}(\theta_{BB}), \tag{22}
\end{aligned}$$

$$\begin{aligned}
408 \quad \phi'_{BA} &= -\gamma\phi_{BA} - \alpha\phi_{BA} + \alpha\phi_{AB} \frac{\Psi''_{AB}(\theta_{AB})}{\Psi'_{AB}(1)} \Psi_{AA}(\theta_{AA}) + \\
409 \quad &\quad \beta_A\phi_{AA} \frac{\Psi'_{AB}(\theta_{AB})}{\Psi'_{AB}(1)} \Psi'_{AA}(\theta_{AA}), \tag{23} \\
410
\end{aligned}$$

411 Consider a node in group A that has i neighbors in A and j neighbors in B.
412 The probability that the node is susceptible is $\theta_{AA}^i \theta_{AB}^j$. The probability that
413 a random node in group A is not infected from A is then $\sum_{i=0}^{\infty} \theta_{AA}^i P_{AA}(i)$,
414 and similarly for infections from B. Thus, the fraction of susceptible nodes

415 in A is

$$416 \quad S_A = \left[\sum_{i=0}^{\infty} \theta_{AA}^i P_{AA}(i) \right] \left[\sum_{j=0}^{\infty} \theta_{AB}^j P_{AB}(j) \right] = \Psi_{AA}(\theta_{AA}) \Psi_{AB}(\theta_{AB}),$$

417 Similarly,

$$418 \quad S_B = \Psi_{BB}(\theta_{BB}) \Psi_{BA}(\theta_{BA}),$$

419 The fractions of infectious individuals in groups A and B change according
420 to

$$421 \quad I'_A = -S'_A - \gamma I_A$$

$$422 \quad = \beta_A \phi_{AA} \Psi'_{AA}(\theta_{AA}) \Psi_{AB}(\theta_{AB}) + \alpha \phi_{AB} \Psi_{AA}(\theta_{AA}) \Psi'_{AB}(\theta_{AB}) - \gamma I_A. \quad (24)$$

$$423 \quad I'_B = -S'_B - \gamma I_B$$

$$424 \quad = \beta_B \phi_{BB} \Psi'_{BB}(\theta_{BB}) \Psi_{BA}(\theta_{BA}) + \alpha \phi_{BA} \Psi_{BB}(\theta_{BB}) \Psi'_{BA}(\theta_{BA}) - \gamma I_B. \quad (25)$$

426 Equations (16)–(25) give the full model. Note that the dynamics of I_A and
427 I_B are determined by the dynamics of θ and ϕ .

428 3.2 Comparison with stochastic simulations

429 To verify our model, we compare the numerical solutions of the model (17)–
430 (25) to stochastic simulations of the underlying epidemic process. Given a
431 network degree distributions for group A, we construct a random network
432 without degree correlation and clustering using the configuration model [2,
433 3, 14]. Specifically, each node is assigned a number of stubs from the given
434 degree distribution, then stubs from two different nodes which are not already
435 neighbors are randomly connected to form an edge; this process is repeated
436 until no stubs can be connected. Group B is constructed similarly. Then
437 each node in A and B is assigned a number of stubs from the AB and BA
438 degree distributions, respectively, and pairs of stubs from A and B are then
439 connected at random to form inter-group edges, until none remain. Notice
440 that the balance condition (15) must be satisfied in the choice of the AB
441 and BA degree distributions. Each node is then labeled with a infection
442 status, i.e., one of susceptible, infectious, and recovered. An infectious node
443 stays infectious for an exponentially distributed time with mean $1/\gamma$, then
444 its status is changed to recovered. A susceptible node stays susceptible for
445 an exponentially distributed time with mean $1/(\beta i)$ where i is the number of

446 its infectious neighbors, then its status is changed to infectious. Recovered
 447 nodes remain recovered. The status of each node is updated until there is
 448 no infectious node or a given terminal time is reached. The simulation is
 449 implemented using the Gillespie algorithm [5, 6].

450 To compare the stochastic simulations with our ODE model (16)–(25),
 451 the degree distributions are fed into the model together with identical initial
 452 infections. The ODE model is then numerically solved, and $I(t) = I_A + I_B$
 453 is compared with the average of the epidemic curves from the stochastic
 454 simulations.

455 Figure 1 shows that, on contact networks with various degree distributions
 456 in groups A and B, the epidemic curves from the ODE model agrees well with
 457 the ensemble averages of the epidemic curves from the stochastic processes.

458 3.3 Basic reproduction number

459 For $i, j = A$ or B , let

$$460 \quad \mathcal{R}_{ij} = \frac{\beta_{ij}}{\beta_{ij} + \gamma} \frac{\Psi''_{ij}(1)}{\Psi'_{ij}(1)},$$

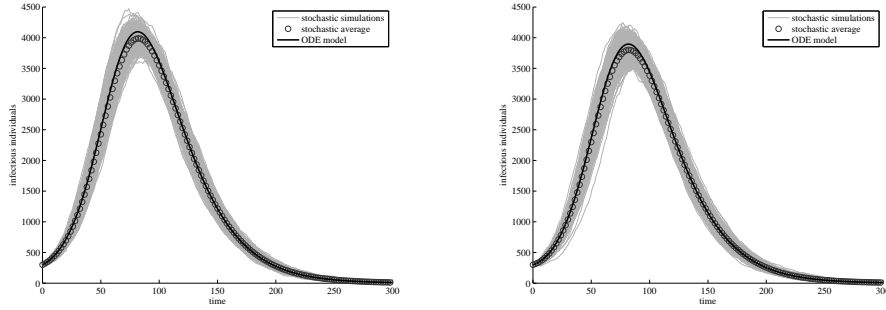
461 and

$$462 \quad r_{ij} = \frac{\beta_{ij}}{\beta_{ij} + \gamma} \Psi'_{ij}(1),$$

463 where $\beta_{AA} = \beta_A$, $\beta_{BB} = \beta_B$, $\beta_{AB} = \beta_{BA} = \alpha$. Note that $\beta_{ij}/(\beta_{ij} + \gamma)$ is the
 464 transmission probability along an edge between Groups i and j . At the be-
 465 ginning of an epidemic, $\Psi''_{ij}(1)/\Psi'_{ij}(1)$ is the average number of transmissible
 466 neighbors in Group j of a newly infected node in Group i that was infected
 467 by a node in Group j , and thus \mathcal{R}_{ij} is the number of secondary infections
 468 in Group j caused by infectious nodes in Group i who have been infected
 469 by ones in Group j . Similarly, r_{ij} is the number of secondary infections in
 470 Group i caused by infectious nodes in Group i who have been infected by
 471 ones *not* in Group j . Thus the matrix

$$472 \quad G = \begin{bmatrix} \mathcal{R}_{AA} & 0 & r_{AB} & 0 \\ 0 & \mathcal{R}_{BB} & 0 & r_{BA} \\ 0 & r_{BB} & 0 & \mathcal{R}_{BA} \\ r_{AA} & 0 & \mathcal{R}_{AB} & 0 \end{bmatrix} \quad (26)$$

473 is the second generation matrix. Its first two rows contain the secondary
 474 infections caused by nodes in group A and B who have been infected by



(a) Poisson random network

(b) Bimodal random network

Figure 1: The epidemic curves of the ODE model (16)–(25) vs the ensemble averages of the stochastic simulations on two random networks: (a) Poisson distributed ($\lambda = 4, 2, 4, 10$ for edge types AA, AB, BB, and BA, respectively), and (b) bimodal (with degrees fixed at 3, 2, 7, 10 for edge types AA, AB, BB, and BA, respectively). The population size of group A is $N_A = 25000$, and group B $N_B = 5000$, transmission rates $\beta_A = \beta_B = \alpha = 0.014$, recovery rate $\gamma = 0.05$. Note that the constraint (15) is satisfied.

475 nodes in the same group, respectively; and the last two rows are for cross-
 476 infected infectious nodes in A and B, respectively.

477 Using the second generation matrix method [16], the basic reproduction
 478 number for the two-group model is computed in Appendix B to be the spec-
 479 tral radius of the matrix G , i.e., $\mathcal{R}_0 = \rho(G)$. In general, this is not equivalent
 480 to Equation (2) because here the network has more structure than a random
 481 network.

482 Note that, when the network is bipartite (i.e., every edge inter-connects
 483 nodes in two groups), \mathcal{R}_{AA} , \mathcal{R}_{BB} , r_{AA} , and r_{BB} all vanish. In this case,

484
$$\mathcal{R}_0 = \sqrt{\mathcal{R}_{AB}\mathcal{R}_{BA}}.$$

485 It is shown in Appendix C Lemma 1 that $\mathcal{R}_0 > \mathcal{R}_{AA}$, $\mathcal{R}_0 > \mathcal{R}_{BB}$, and
 486 $\mathcal{R}_0 > \sqrt{\mathcal{R}_{AB}\mathcal{R}_{BA}}$, i.e., \mathcal{R}_0 is larger than the basic reproduction number of
 487 the disease when restricted to each component.

488 Assume that each type of edge is randomly removed (by choosing a node
 489 randomly then removing a random edge from that node), and this may occur
 490 with different rates for each type. Then the random edge removal model (4)–
 491 (5) describes the evolution for the degree distribution for each type of edge.
 492 From Appendix A, $\langle k \rangle = \Psi'_{ij}(1)$ and $\langle k^2 \rangle / \langle k \rangle = \Psi''_{ij}(1) / \Psi'_{ij}(1)$ for all $i, j = A$
 493 and B decrease with edge removal. In Appendix C it is shown that, because
 494 of this,

$$495 \quad \frac{d}{d\tau} \mathcal{R}_0 < 0$$

496 with edge removal. As a special case, removing edges from any part of the
 497 network reduces \mathcal{R}_0 .

498 4 Discussion and Conclusions

499 It would appear obvious that in any population if the total number of po-
 500 tentially disease-causing contacts were to drop before an epidemic (say, as a
 501 result of vaccinations and the closing down of public places), so should the
 502 basic reproduction number. This follows from reasoning that if the average
 503 individual has fewer contacts, then the disease has fewer channels available
 504 by which to spread. Indeed, we proved in Section 2 that if the edge removal
 505 process is truly random, as given by the system of differential equations (4)
 506 and (5), then the basic reproduction number \mathcal{R}_0 decreases, as expected, when
 507 edges are removed.

508 In contrast, the mathematical arguments in the introduction seemed to
 509 indicate that for certain networks, we may see the opposite effect. In the case
 510 of a simple bimodal degree distribution, we described schemes for modifying
 511 the network in such a way that the average degree decreases, yet \mathcal{R}_0 as
 512 defined by (2) increases. Apparently all that is required is an edge-deletion
 513 process that causes either a tandem decrease in both the low degree k_1 and
 514 the high degree k_2 , or a decrease in k_1 while k_2 remains fixed.

515 The reason for the “paradox” becomes clear if we pay closer attention
 516 to the definition of the basic reproduction number. The calculations from
 517 the introduction make use of the fact that for a random contact network
 518 of configuration type the basic reproduction number \mathcal{R}_0 is defined in (2).

519 However, as already indicated in the introduction, once we begin to remove
520 edges subject to constraints the network changes character. Say, for example,
521 we are ensuring that k_1 and k_2 change (or stay fixed) in a very particular
522 way. To accomplish this, the edge deletion process must be selective rather
523 than haphazard, and thus the network is no longer of the configuration type.

524 The \mathcal{R}_0 defined in (2) applies to networks which are randomly constructed
525 from a given degree distribution. So by artificially manipulating the degree
526 distribution, we in fact simulate a reconstruction of the network, rather than
527 simple edge deletion. For this reason we cannot use this formula to illustrate
528 a before and after picture of the basic reproduction number in networks which
529 have had a few edges selectively deleted, but are otherwise structurally the
530 same. In fact we are modeling a reorganization of the network, where the
531 degree distribution is altered slightly and then the entire network is rebuilt.

532 As an example, consider the reorganization of a bimodal network where
533 k_1 decreases and k_2 stays fixed. Imagine trying to decrement the degree of
534 a low-degree node, chosen at random. We are required to select one of its
535 edges and delete it. However, it is forbidden to remove edges belonging to a
536 high-degree node. So if it happens that a high-to-low edge is selected, only
537 the low-degree half may be discarded. The other half, a stub belonging to
538 the high-degree node, must be reconnected somewhere else. The only way to
539 “find a node” for it is to identify a second to-be-removed high-to-low edge,
540 discard the low-degree half and then connect the leftover high degree stubs
541 together, thus creating a new high-to-high edge. In this way we are reducing
542 the average degree, while leaving k_2 fixed, as intended. However, in the
543 end we have increased the proportion of edges that link high-degree nodes
544 together, and the effect of this restructuring seems to outweigh the effect of
545 a reduction in $\langle k \rangle$ for certain choices of k_1 and k_2 . In a roundabout way,
546 this illustrates the relative importance of connections amongst high-degree
547 individuals to the spread of disease on networks.

548 The key point is, of course, that the definition of \mathcal{R}_0 in (2) loses its
549 meaning once we introduce changes to the network that render the network
550 “non-random”. At that point one needs a different definition for a basic
551 reproduction number.

552 To incorporate nonuniform edge removal, in Section 3, we extended the
553 Miller model [11] model for a contact network consisting two groups of nodes
554 with random intra- and inter-group connections; the transmission rates may
555 differ inside and between the different parts of the network; the edges could
556 be randomly removed from any part of the network. We then derive the basic

557 reproduction number as appropriate for this scenario, and were able to show
 558 that \mathcal{R}_0 will always decrease under edge removal. However this model may
 559 not be suitable for dividing a random network into two subgroups, because
 560 the resulting inter-group degree distributions may be correlated to intra-
 561 degree distributions, as confined by the total degree distribution (unless for
 562 a Poisson random network). On the other hand, this model can be extended
 563 to such cases by deriving the inter-group degree distribution from the total
 564 degree distribution and intra-degree distributions.

565 Most importantly, the dynamical system approach for the evolution of de-
 566 gree distribution under random edge removal allows us to estimate the point
 567 at which \mathcal{R}_0 drops below unity along the edge removal dynamics. That is, it
 568 tells us how many edges must be randomly removed to curtail an epidemic.

569 **Acknowledgements** This research is supported by NSERC Discovery grants
 570 (JM and RI), and University of Victoria (DK). We wish to express our grati-
 571 tude to the referees, whose comments led to revisions which clarified matters
 572 and improved the paper.

573 **A The rate of change of the basic reproduc-** 574 **tion number**

575 The expression 7 is obtained as follows. From Equation (6), the rate of
 576 change of \mathcal{R}_0 along solutions to Equations (4) and (5) is

$$577 \quad \frac{d}{d\tau} \left(T \frac{\sum_{k=0}^{\infty} k^2 N_k}{\sum_{k=0}^{\infty} k N_k} \right) = T \left(\frac{\sum_{k=0}^{\infty} k^2 N'_k}{L} - \frac{(\sum_{k=0}^{\infty} k^2 N_k)(\sum_{k=0}^{\infty} k N'_k)}{L^2} \right) \quad (27)$$

578 We substitute (4) in place of the N'_k terms. Notice that because of the
 579 coefficients k and k^2 , all of the N'_0 terms vanish in this substitution. We first

580 compute

$$\begin{aligned}
581 \quad & \frac{1}{L} \sum_{k=0}^{\infty} k^2 N'_k \\
582 \quad &= \frac{1}{L(N - N_0)} \sum_{k=0}^{\infty} k^2 (N_{k+1} - N_k) + \frac{1}{L^2} \sum_{k=0}^{\infty} k^2 [(k+1)N_{k+1} - kN_k] \\
583 \quad &= \frac{1}{L(N - N_0)} \sum_{k=1}^{\infty} [(k-1)^2 N_k - k^2 N_k] + \frac{1}{L^2} \sum_{k=1}^{\infty} [k(k-1)^2 N_k - k^3 N_k] \\
584 \quad &= \frac{1}{L(N - N_0)} \sum_{k=1}^{\infty} (1-2k)N_k + \frac{1}{L^2} \sum_{k=1}^{\infty} k(1-2k)N_k \\
585 \quad &= \frac{2}{L} - \frac{2}{N - N_0} - \frac{2}{L^2} \sum_{k=1}^{\infty} k^2 N_k . \\
586 \quad &
\end{aligned}$$

587 Then we compute

$$\begin{aligned}
588 \quad & \sum_{k=0}^{\infty} k N'_k = \frac{1}{N - N_0} \sum_{k=0}^{\infty} k (N_{k+1} - N_k) + \frac{1}{L} \sum_{k=0}^{\infty} [k(k+1)N_{k+1} - k^2 N_k] \\
589 \quad &= \frac{1}{N - N_0} \sum_{k=1}^{\infty} [(k-1)N_k - kN_k] + \frac{1}{L} \sum_{k=1}^{\infty} [k(k-1)N_k - k^2 N_k] \\
590 \quad &= -\frac{1}{N - N_0} \sum_{k=1}^{\infty} N_k - \frac{1}{L} \sum_{k=1}^{\infty} k N_k \\
591 \quad &= -2 . \\
592 \quad &
\end{aligned}$$

593 Thus,

$$594 \quad \frac{1}{L^2} \left(\sum_{k=0}^{\infty} k^2 N_k \right) \left(\sum_{k=0}^{\infty} k N'_k \right) = -\frac{2}{L^2} \sum_{k=0}^{\infty} k^2 N_k .$$

595 It thus follows that

$$\begin{aligned}
596 \quad & \frac{d}{d\tau} \mathcal{R}_0 = T \left[\frac{2}{L} - \frac{2}{N - N_0} - \frac{2}{L^2} \sum_{k=1}^{\infty} k^2 N_k + \frac{2}{L^2} \sum_{k=0}^{\infty} k^2 N_k \right] \\
597 \quad &= 2T \left(\frac{1}{L} - \frac{1}{N - N_0} \right) . \\
598 \quad &
\end{aligned}$$

599 Note that

$$600 \quad \frac{1}{L} - \frac{1}{N - N_0} = \frac{1}{\sum_{k=1}^{\infty} k N_k} - \frac{1}{\sum_{k=1}^{\infty} N_k} < 0.$$

601 Thus,

$$602 \quad \frac{d}{d\tau} \mathcal{R}_0 < 0.$$

603 **B The basic reproduction number of the two-** 604 **group model**

605 To compute the basic reproduction number \mathcal{R}_0 for the two-group model (16)–
606 (21), we employ the second generation matrix method [16]. This method
607 identifies \mathcal{R}_0 as the dominant eigenvalue of the second generation matrix
608 FV^{-1} . Here, for a general disease model with some susceptible and infected
609 classes at the disease, we restrict our attention to the infected classes about
610 the disease free equilibrium. The matrix F is the new infection matrix, whose
611 ij entry is the rate of new infections entering class j caused by class i , and V
612 is the transition matrix whose ij entry is the rate at which class i transfers to
613 class j . And thus the ij entry of V^{-1} is the amount of time staying in class i
614 starting from class j . This implies that the ij entry of the second generation
615 matrix FV^{-1} is the average number of secondary infections in class i caused
616 by class j . For our model, the ϕ classes are treated as “infected” classes.

617 To determined the matrices F and V , we linearize (17)–(23) about the
618 disease-free equilibrium ($\phi_{AA} = \phi_{BB} = \phi_{AB} = \phi_{BA} = 0$ and $\theta_{AA} = \theta_{BB} =$
619 $\theta_{AB} = \theta_{BA} = 1$) to get

$$620 \quad \dot{\phi}_{AA} = -(\beta_A + \gamma)\phi_{AA} + \beta_A\phi_{AA}\frac{\Psi''_{AA}(1)}{\Psi'_{AA}(1)} + \alpha\phi_{AB}\Psi'_{AB}(1)$$

$$621 \quad \dot{\phi}_{BB} = -(\beta_B + \gamma)\phi_{BB} + \beta_B\phi_{BB}\frac{\Psi''_{BB}(1)}{\Psi'_{BB}(1)} + \alpha\phi_{BA}\Psi'_{BA}(1)$$

$$622 \quad \dot{\phi}_{AB} = -(\alpha + \gamma)\phi_{AB} + \alpha\phi_{BA}\frac{\Psi''_{BA}(1)}{\Psi'_{BA}(1)} + \beta_B\phi_{BB}\Psi'_{BB}(1)$$

$$623 \quad \dot{\phi}_{BA} = -(\alpha + \gamma)\phi_{BA} + \alpha\phi_{AB}\frac{\Psi''_{AB}(1)}{\Psi'_{AB}(1)} + \beta_A\phi_{AA}\Psi'_{AA}(1)$$

624

625 In matrix form, this is

$$626 \quad \frac{d}{dt} \begin{bmatrix} \phi_{AA} \\ \phi_{BB} \\ \phi_{AB} \\ \phi_{BA} \end{bmatrix} = (F - V) \begin{bmatrix} \phi_{AA} \\ \phi_{BB} \\ \phi_{AB} \\ \phi_{BA} \end{bmatrix}.$$

627 Here the terms related to new infections give

$$628 \quad F = \begin{bmatrix} \beta_A \frac{\Psi''_{AA}(1)}{\Psi'_{AA}(1)} & 0 & \alpha \Psi'_{AB}(1) & 0 \\ 0 & \beta_B \frac{\Psi''_{BB}(1)}{\Psi'_{BB}(1)} & 0 & \alpha \Psi'_{BA}(1) \\ 0 & \beta_B \Psi'_{BB}(1) & 0 & \alpha \frac{\Psi'_{BA}(1)}{\Psi'_{BA}(1)} \\ \beta_A \Psi'_{AA}(1) & 0 & \alpha \frac{\Psi''_{AB}(1)}{\Psi'_{AB}(1)} & 0 \end{bmatrix},$$

629 and the terms not related to new infections give

$$630 \quad V = \begin{bmatrix} \beta_A + \gamma & 0 & 0 & 0 \\ 0 & \beta_B + \gamma & 0 & 0 \\ 0 & 0 & \alpha + \gamma & 0 \\ 0 & 0 & 0 & \alpha + \gamma \end{bmatrix}.$$

631 Thus, FV^{-1} is the matrix specified in (26), and the basic reproduction num-
632 ber is its spectral radius.

633 C The monotonicity of the basic reproduc- 634 tion number of the two-group model

635 The characteristic equation of this matrix is a fourth order polynomial

$$636 \quad f(x) = (\mathcal{R}_{AA} - x)[(\mathcal{R}_{BB} - x)(x^2 - R_{AB}\mathcal{R}_{BA}) + r_{BB}\mathcal{R}_{AB}r_{BA}] + \\ 637 \quad r_{AA}r_{AB}[(\mathcal{R}_{BB} - x)\mathcal{R}_{BA} - r_{BB}r_{BA}] \\ 638 \quad = 0. \tag{28}$$

640 The basic reproduction number \mathcal{R}_0 is thus the the largest root of $f(x) = 0$.

641 **Lemma 1.** $\mathcal{R}_0 > \mathcal{R}_{AA}$, $\mathcal{R}_0 > \mathcal{R}_{BB}$, and $\mathcal{R}_0 > \sqrt{\mathcal{R}_{AA}\mathcal{R}_{BB}}$.

642 *Proof.* Because of the symmetry of the system on A and B, i.e., exchanging
643 A and B yields the same system, without loss of generality, we assume that
644 $\mathcal{R}_{AA} \geq \mathcal{R}_{BB}$ (otherwise, we switch A and B in the proof).

$$645 \quad f(\mathcal{R}_{AA}) = r_{AA}r_{AB}[(\mathcal{R}_{BB} - \mathcal{R}_{AA})\mathcal{R}_{BA} - r_{BB}r_{BA}] < 0$$

646 because both terms in the bracket are negative. Note that $f(\infty) = \infty$. Thus,
647 the largest root of $f(x)$ satisfies $\mathcal{R}_0 > \mathcal{R}_{AA}$. Because of symmetry on A and
648 B, $\mathcal{R}_0 > \mathcal{R}_{BB}$. Since $f(\mathcal{R}_0) = 0$, from (28),

$$649 \quad \mathcal{R}_0^2 - \mathcal{R}_{AB}\mathcal{R}_{BA} = \frac{(\mathcal{R}_0 - \mathcal{R}_{AA})r_{BB}\mathcal{R}_{AB}r_{BA}}{(\mathcal{R}_{AA} - \mathcal{R}_0)(\mathcal{R}_{BB} - \mathcal{R}_0)} +$$

$$650 \quad \frac{r_{AA}r_{AB}[(\mathcal{R}_0 - \mathcal{R}_{BB})\mathcal{R}_{BA} + r_{BB}r_{BA}]}{(\mathcal{R}_{AA} - \mathcal{R}_0)(\mathcal{R}_{BB} - \mathcal{R}_0)}.$$

652 Note that each term on the right hand side is positive because $\mathcal{R}_0 > \mathcal{R}_{AA}$
653 and $\mathcal{R}_0 > \mathcal{R}_{BB}$. Thus, $\mathcal{R}_0 > \sqrt{\mathcal{R}_{AA}\mathcal{R}_{BB}}$. \square

654 As stated in Section 3, when the four types of edges are randomly removed
655 (possibly with different rates), for all $i, j = A$ and B , $\frac{d}{d\tau}\mathcal{R}_{ij} < 0$ and $\frac{d}{d\tau}r_{ij} < 0$
656 with edge removal (where, as in Section 2, τ is the time in the edge removal
657 process). We differentiate the expression $f(\mathcal{R}_0) = 0$ with respect to τ , which
658 is equivalent to the number of edges removed, to investigate how \mathcal{R}_0 changes

659 under this process. The multivariable chain rule gives

$$\begin{aligned}
660 \quad \frac{d}{d\tau}\mathcal{R}_0 &= -\mathcal{R}'_{AA} \frac{(\mathcal{R}_{BB} - \mathcal{R}_0)(\mathcal{R}_0^2 - R_{AB}\mathcal{R}_{BA}) + r_{BB}\mathcal{R}_{AB}r_{BA}}{f'(\mathcal{R}_0)} \\
661 &\quad -\mathcal{R}'_{BB} \frac{(\mathcal{R}_{AA} - \mathcal{R}_0)(\mathcal{R}_0^2 - R_{AB}\mathcal{R}_{BA}) + r_{AA}\mathcal{R}_{BA}r_{AB}}{f'(\mathcal{R}_0)} \\
662 &\quad -\mathcal{R}'_{AB} \frac{[-\mathcal{R}_{BA}(\mathcal{R}_{BB} - \mathcal{R}_0) + r_{BB}r_{BA}](R_{AA} - R_0)}{f'(\mathcal{R}_0)} \\
663 &\quad -\mathcal{R}'_{BA} \frac{[-\mathcal{R}_{AB}(\mathcal{R}_{AA} - \mathcal{R}_0) + r_{AA}r_{AB}](R_{BB} - R_0)}{f'(\mathcal{R}_0)} \\
664 &\quad -r'_{AA} \frac{r_{AB}[(\mathcal{R}_{BB} - \mathcal{R}_0)\mathcal{R}_{BA} - r_{BB}r_{BA}]}{f'(\mathcal{R}_0)} \\
665 &\quad -r'_{BB} \frac{r_{BA}[(\mathcal{R}_{AA} - \mathcal{R}_0)\mathcal{R}_{AB} - r_{AA}r_{AB}]}{f'(\mathcal{R}_0)} \\
666 &\quad -r'_{AB} \frac{r_{AA}[(\mathcal{R}_{BB} - \mathcal{R}_0)\mathcal{R}_{BA} - r_{BB}r_{BA}]}{f'(\mathcal{R}_0)} \\
667 &\quad -r'_{BA} \frac{r_{BA}[(\mathcal{R}_{AA} - \mathcal{R}_0)\mathcal{R}_{AB} - r_{AA}r_{AB}]}{f'(\mathcal{R}_0)}. \\
668
\end{aligned}$$

669 Because \mathcal{R}_0 is the largest root of $f(x)$, which is a fourth order polynomial
670 opening upward, $f'(\mathcal{R}_0) > 0$. Again, because $\mathcal{R}_0 \geq \mathcal{R}_{AA}$ and $\mathcal{R}_0 \geq \mathcal{R}_{BB}$,
671 the last six fractions are all negative. And since $f(\mathcal{R}_0) = 0$,

$$\begin{aligned}
672 & \\
673 \quad & (\mathcal{R}_{BB} - \mathcal{R}_0)(\mathcal{R}_0^2 - R_{AB}\mathcal{R}_{BA}) + r_{BB}\mathcal{R}_{AB}r_{BA} \\
674 & \quad = -\frac{r_{AA}r_{AB}[(\mathcal{R}_{BB} - \mathcal{R}_0)\mathcal{R}_{BA} - r_{BB}r_{BA}]}{\mathcal{R}_{AA} - \mathcal{R}_0} < 0. \\
675 &
\end{aligned}$$

676 Similarly.

$$677 \quad (\mathcal{R}_{BB} - \mathcal{R}_0)(\mathcal{R}_0^2 - R_{AB}\mathcal{R}_{BA}) + r_{BB}\mathcal{R}_{AB}r_{BA} < 0.$$

678 Thus, the coefficients of all \mathcal{R}_{ij} and r_{ij} for $i, =A$ and B are all positive. This
679 implies that, if all the derivatives $\mathcal{R}'_{ij} \leq 0$ and $r'_{ij} \leq 0$, and at least one is
680 strictly negative, then

$$681 \quad \frac{d}{d\tau}\mathcal{R}_0 < 0.$$

References

- 682
- 683 [1] F. Ball and P. Neal. Network epidemic models with two levels of mixing.
684 *Math. Biosci.*, 212:69–87, 2008.
- 685 [2] A. Bekessy, P. Bekessy, and J. Komlos. Asymptotic enumeration of reg-
686 ular matrices. *Studia Scientiarum Mathematicarum Hungarica*, 7:343–
687 353, 1972.
- 688 [3] E. A. Bender and E. R. Canfield. The asymptotic number of labelled
689 graphs with given degree sequences. *Journal of Combinatorial Theory*
690 *(A)*, 24:296–307, 1978.
- 691 [4] S. P. Ellner and J. Guckenheimer. *Dynamic Models in Biology*. Princeton
692 University Press, 2006.
- 693 [5] D. T. Gillespie. A general method for numerically simulating the
694 stochastic time evolution of coupled chemical reactions. *Journal of Com-*
695 *putational Physics*, 22:403–434, 1976.
- 696 [6] D. T. Gillespie. Exact stochastic simulation of coupled chemical reac-
697 tions. *The Journal of Physical Chemistry*, 81:2340–2361, 1977.
- 698 [7] W. O. Kermack and A. G. McKendrick. A contribution to the mathe-
699 matical theory of epidemics. *Proceedings of Royal Society of London A*,
700 115:700721, 1927.
- 701 [8] J. Lindquist, J. Ma, P. van den Driessche, and F. H. Willeboordse.
702 Network evolution by different rewiring schemes. *Physica D*, 238:370–
703 378, 2009.
- 704 [9] J. Lindquist, J. Ma, P. van den Driessche, and F. H. Willeboordsde.
705 Effective degree network disease models. *J. Math. Biol.*, 62:143–164,
706 2010.
- 707 [10] R. M. May, R. M. Anderson, and M. E. Irwin. The transmission dy-
708 namics of human immunodeficiency virus (HIV). *Phil. Trans. R. Soc.*
709 *Lond. B*, 321:565–607, 1988.
- 710 [11] J. Miller. A note on a paper by erik volz: Sir dynamics in random
711 networks. *Journal of Mathematical Biology*, 62:349–358, 2011.

- 712 [12] J. C. Miller. A note on a paper by Erik Volz: SIR dynamics in random
713 networks. *J. Math. Biol.*, 62:349–358, 2011.
- 714 [13] M. E. J. Newman. Spread of epidemic disease on networks. *Phys. Rev.*
715 *E*, 66:016128, 2002.
- 716 [14] M. E. J. Newman, S. H. Strogatz, and D. J. Watts. Random graphs with
717 arbitrary degree distributions and their applications. *Physical Review*
718 *E*, 64:026118, 2001.
- 719 [15] R. Pastor-Satorras and A. Vespignani. Epidemic dynamics in finite size
720 scale-free networks. *Phys. Rev. E*, 65(035108(R)), 2002.
- 721 [16] P. van den Driessche and J. Watmough. Reproduction numbers and
722 sub-threshold endemic equilibria for compartmental models of disease
723 transmission. *Mathematical Biosciences*, 180:29–48, 2002.
- 724 [17] E. M. Volz. SIR dynamics in random networks with heterogeneous con-
725 nectivity. *J. Math. Biol.*, 56:293–310, 2008.